URSI - RCRS 2022, IIT (Indore), India, 1 - 4 December, 2022

Antenna Array Ambiguity Function Based Study of Integration Effect on a 2D Automotive MIMO RADAR Antenna Placed Behind a Painted Bumper

Jogesh Chandra Dash, Debdeep Sarkar
Indian Institute of Science, Bangalore, India, https://ece.iisc.ac.in/ debdeeps/

Abstract

In this paper, we study the integration effects of a 2D MIMO RADAR antenna for automotive applications, placed behind a painted bumper. First, a 3Tx-4Rx 2D-MIMO RADAR antenna system is designed, where the individual Tx/Rx antenna is a seven-element series-fed modified binomial array configuration having side-lobe level less than 16 dB and 80^0 azimuth field-of-view (FoV). Then the 2D MIMO RADAR antenna is placed behind a simplified curved bumper having two paint layers, and the antenna-painted bumper integration effects are studied via the S-parameter response and antenna array ambiguity function (AAAF) model. Both the AAAF and S-parameter analysis provide key insights into the comparative performance of 1D and 2D MIMO RADARs integrated with bumpers, which can help determine possible corrective measures in real-time applications.

1 Introduction

Autonomous vehicles have gained tremendous attention these days and with this surge, various technologies have also come to the fore that caters to the demand for active safety and to avoid human errors while driving. Advanced driver assistance system (ADAS) is one such technology that facilitates a wide range of functionalities such as adaptive cruise control (ACC), parking assistance, blind spot detection, surrounding view, pedestrian detection, etc. As the degree of automation has reached levels 4 and 5 [1], situational sensing is an utmost priority, necessitating sensor technologies [2] with high-resolution mapping. Generally, this high-resolution sensing is achieved by using various sensors such as LIDAR, camera, ultrasonic SONAR, and automotive RADAR. The optical sensors such as LIDAR and camera provide high angular resolution and visual representation of the target respectively but fail in low light conditions and face high attenuation in bad weather conditions such as rain, fog, dust, snow, etc [3]. The SONAR sensor is suitable for low-speed and short-range target avoidance, however, its spatial resolution and maximum range are restricted for dynamic driving conditions and at the same time get attenuated in adverse weather conditions. On the other hand, RADAR is one of the most efficient sensors among others which is unaffected by weather conditions and independent of lighting conditions. Moreover, accurate velocity estimation and moving target detection using the Doppler effect are the key differentiators of the RADAR from other sensors. Therefore, RADAR is the most decorated sensor for an autonomous vehicle. However, the angular resolution of the conventional RADAR is less compared to optical sensors and it is inversely proportional to the antenna size. Here, the MIMO technology in the RADAR system provides a degree of freedom to improve the angular resolution without increasing the physical antenna aperture.

The MIMO technique increases the RADAR angular resolution by introducing the formation of a virtual array of receiver antenna that contains more number of antenna elements and a larger virtual aperture than the physical antenna through the use of waveform diversity (i.e., transmitting orthogonal waveform from transmitter antennas) [4]. MIMO RADAR comes in three different configurations such as long-range, medium-range, and short-range RADAR based on maximum attainable range and field-of-view (FoV) and is widely used in the 77 GHz band. Nevertheless, the practical problem arises when these RADARs are mounted behind a bumper of an autonomous vehicle having six-to-seven layers of paint material [5]. This painted bumper introduces additional loss in the transmission/reception and affects the direction-of-arrival (DoA) estimation and RADAR resolution.

In this paper, we use the antenna array ambiguity function (AAAF) model and the S-parameter response to provide intuition into the effect of an antenna-painted bumper integrated system. Initially, the paper provides insight on 1D and 2D MIMO RADAR antenna design and studies the angular resolution provided by the antenna configurations. All the designs and simulations in this manuscript are carried out using CST Microwave Studio.

2 1D and 2D MIMO RADAR Antenna Design

The schematic of 2Tx-4Rx 1D and 3Tx-4Rx 2D MIMO RADAR antenna are shown in Fig. 1 and Fig. 2 respectively. The antennas are designed at 77 GHz automotive RADAR operating band on a 0.25 mm thick Roger 5880LZ

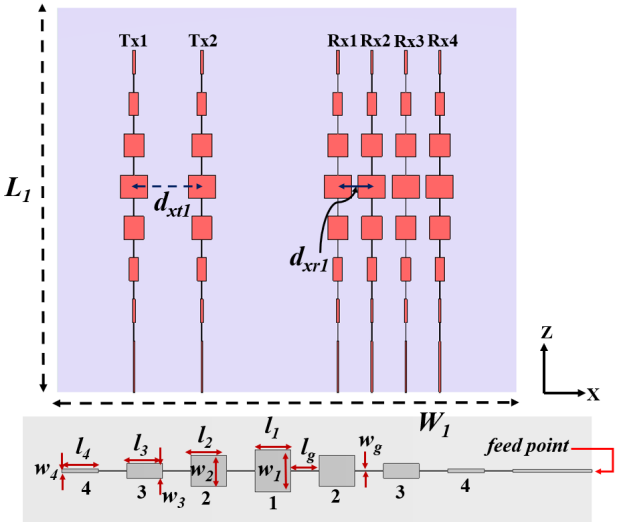

Figure 1. Schematic of 2Tx-4Rx 1D MIMO RADAR antenna. Individual antenna dimension in mm: $l_1 = 1.35, w_1 = 1.6, l_2 = 1.35, w_2 = 1.185, l_3 = 1.36, w_3 = 0.553, l_4 = 1.39, w_4 = 0.185, l_g = 1.085, w_g = 0.03, d_{xt1} = 3.9, d_{yr1} = 2, L_1 = 22.7, W_1 = 27$.

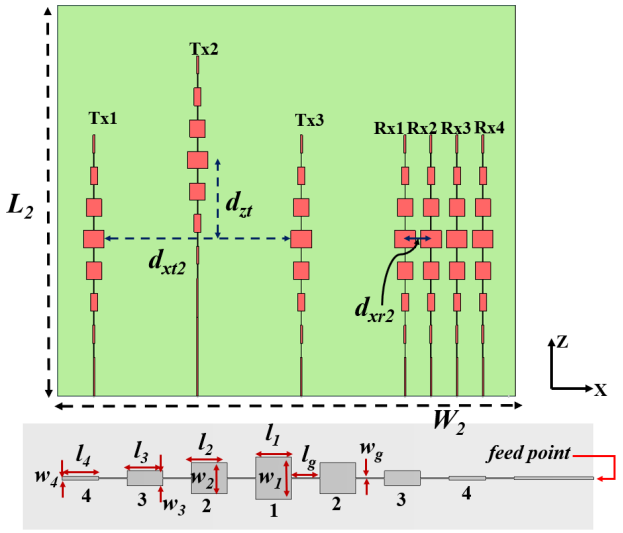

Figure 2. Schematic of 3Tx-4Rx 2D MIMO RADAR antenna. Individual antenna dimension in mm: $l_1 = 1.35, w_1 = 1.6, l_2 = 1.35, w_2 = 1.185, l_3 = 1.36, w_3 = 0.553, l_4 = 1.39, w_4 = 0.185, l_g = 1.085, w_g = 0.03, d_{xt2} = 16, d_{zt} = 6.1, d_{yr2} = 2, L_2 = 30.14, W_2 = 37.3$.

material ($\varepsilon_r = 2, tan\delta = 0.0021$). The individual antenna element of these two MIMO configurations is a modified binomial tapered series-fed array [6], where the design parameters are listed in Fig. 1 and 2. It can be seen that the Tx2 in Fig. 2 is extended by $d_{tz} = 1.5\lambda_0$ (λ_0 is the free space wavelength at 77 GHz frequency) distance towards the z-direction to get a 2D MIMO antenna design. It is also taken care that the extension made in Tx2 maintains the 77 GHz resonance as shown in the S-parameter curve in Fig. 3(a). Fig. 3(b) shows the 3D-radiation pattern of the showing 11.5 dBi broadside gain having sidelobe level (SLL) less than 16 dB and 80^0 FoV.

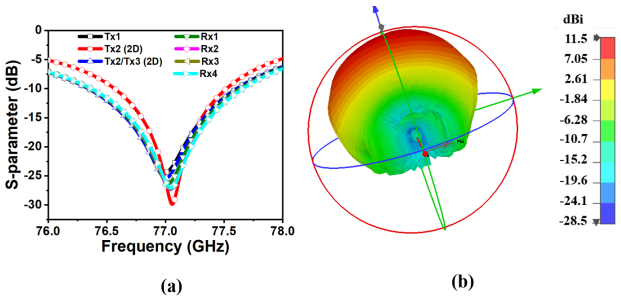

Figure 3. (a) Variation of S-parameter over frequency for all antenna elements and (b) 3D radiation pattern at 77 GHz of Tx2 showing gain of 2D MIMO RADAR antenna configuration shown in Fig. 1.

Though the antenna type and arrangement for 1D and 2D MIMO RADAR configurations are looking similar, the offset design of Tx2 in Fig. 2 creates the actual difference between 1D and 2D MIMO by providing an additional degree of freedom in elevation plane resolution. More studies on 1D MIMO RADAR antenna and bumper integration effects are provided in our earlier works [7], [8]. Now, the antenna arrangement for the proposed 1D and 2D MIMO RADAR antennas can be expressed as (1) and (2) respectively,

$$x-\text{direction}: M_t = [0, \lambda_0], M_r = [3\lambda_0, 3.5\lambda_0, 4\lambda_0, 4.5\lambda_0] \quad (1)$$

$$(x,z)-\text{plane}: M_t = [(0,0),(2\lambda_0, 1.565\lambda_0),(4\lambda_0,0)], \\ M_r = [(6\lambda_0,0),(6.5\lambda_0,0),(7\lambda_0,0),(7.5\lambda_0,0)] \quad (2)$$

Here M_t and M_r are the position vectors of transmitter and receiver arrays. The antenna arrangement for (1) provides a 1D virtual aperture $d_x = 5.5\lambda_0$. According to the Rayleigh criterion [9], the angular resolution provided by 1D MIMO RADAR in azimuth is $\Delta\varphi_x = 1.22\lambda_0/d_x = 12.7^0$. On the other hand, 2D MIMO RADAR generates a 2D virtual array [10] along $xz-$plane. The schematic of 2D virtual array representation is discussed in [11]. The 2D virtual array, due to the proposed 2D MIMO RADAR antenna, generates array sparsity [12] with 8 elements having azimuth aperture $d_x = 11.5\lambda_0$ along with an elevation aperture $d_y = 1.565\lambda_0$. Similarly, according to the Rayleigh criterion the angular resolution provided by 2D MIMO RADAR in azimuth and elevation are $\Delta\varphi_x = 1.22\lambda_0/d_x = 6.07^0$ and $\Delta\varphi_x = 1.22\lambda_0/d_y = 44.8^0$ respectively. The overall footprint (i.e. occupied area) of the 2D MIMO RADAR is nearly 1.73 times the 1D MIMO RADAR. However, the proposed 2D MIMO RADAR not only improves the azimuth resolution but also provides elevation resolution, unlike the 1D MIMO RADAR.

.

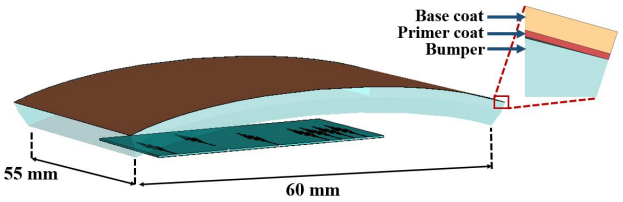

Figure 4. Schematic of 2D MIMO RADAR antenna-painted bumper integrated system.

3 Integration of 1D and 2D MIMO RADAR antenna Behind a Painted Bumper

Next the MIMO RADAR is integrated with a simplified curved bumper model having $\varepsilon_r = 2$ and $tan\delta = 0.01$. The physical dimension of the bumper is taken as $55 \times 60\text{mm}^2$ such that it can surround the proposed MIMO RADAR antenna. As mentioned earlier, the automotive industries generally use six-to-seven layers of painted material for vehicle aesthetics. Here, we have considered only two paint materials for the study purpose. A primer coat ($\varepsilon_r = 9, tan\delta = 0.06$) and a base coat ($\varepsilon_r = 9.99, tan\delta = 0.907$), having thicknesses 4μm and 15μm respectively, are applied on the bumper [13]. Fig. 4 shows the schematic of the antenna-bumper integrated system. The bumper thickness is varied from 2.75mm at the corner to 3mm at the center.

The S-parameter response for the 2D MIMO RADAR antenna without and with the painted bumper is computed to observe the effect of integration. Fig. 5 shows the S-parameter response for Tx1 of 2D MIMO along with the mutual coupling effect with other antennas. Note that, S-parameter response for only one antenna is considered here to provide clarity in the response and similar effects are also observed in the S-parameter response of other antennas in the proposed 2D MIMO RADAR antenna configuration. The antenna without any integration shows perfect $|S_{11}|$ response at 77 GHz and the minimum mutual coupling between the other antennas is below -30 dB (see Fig. 5(a)). Fig. 5(b) shows the S-parameter response when only bumper material is placed above the antenna, which shows a deviation in the $|S_{11}|$ curve and an increase in the minimum mutual coupling near -30 dB. The antenna with the painted bumper in Fig. 5(c) and (d) shows a further increase in minimum mutual coupling above -30 dB with the deviated $|S_{11}|$ response from the 77 GHz operating frequency. This variation in the S-parameter response is due to the multi-path reflections of radiated electromagnetic waves between the antenna and bumper. This reduces the antenna impedance matching at the desired operating frequency and eventually reduces the maximum power transfer to the antenna element and affect antenna radiation efficiency.

In addition, for a RADAR problem, an unambiguous estimation of direction-of-arrival (DoA) is the fundamental requirement. Ambiguity in DoA estimation, due to the presence of a painted bumper, may lead to the miss of target position and consequently lead to detrimental effects. There-

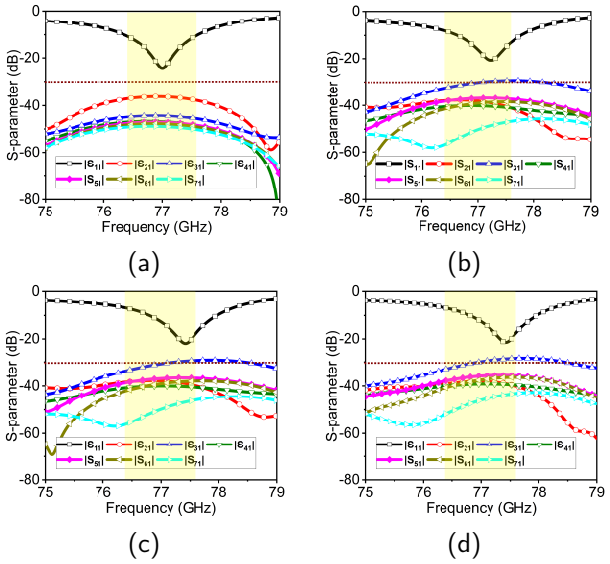

Figure 5. Variation of S-parameters with frequency for Tx1-antenna of the proposed 2D-MIMO RADAR antenna (Fig. 2) (a)without bumper, (b) with bumper, (c)with bumper+ primer coat, and (d)with bumper+ primer coat+ base coat.

fore, to study the effect of the integrated bumper-MIMO RADAR systems, here the AAAF is used which provides information on ambiguity in DoA and angular resolution. Mathematically, AAAF $\chi(\psi_i, \psi_j)$ can be represented as (3) [14]

$$\chi(\psi_i, \psi_j) = \frac{|Y^H(\psi_i).Y(\psi_j)|}{||Y(\psi_i)||.||Y(\psi_j)||} \tag{3}$$

Where Y represents virtual array steering vector, $(.)^H$ represents the Hermitian operator, $||.||$ represents the norm operator and $0 \leq \psi_i, \psi_j \leq 2\pi$. More details about AAAF and relevant mathematical formulation to compute are provided in [8], [14]. The computed AAAF plot for both 1D and 2D MIMO RADAR antenna is shown in Fig. 6 for various combinations of the antenna and pained bumper; where all the left-side plots such as (a1), (b1), (c1), and (d1) belong to 1D and right-side plots such as (a2), (b2), (c2), and (d2) belong to 2D MIMO. The diagonal length and width of the AAAF plot signifies the FoV and angular resolution of the MIMO RADAR antenna. From the very initial observation, it can be seen in Fig. 6 that the thinner diagonal width of AAAF plots for the proposed 2D MIMO compared to the 1D MIMO. This signifies the improved angular resolution of the proposed 2D MIMO antenna configuration compared to 1D, which is consistent with the discussion on angular resolution in section II. In addition, the key observation can be drawn from Fig. 6 that standalone antennas exhibit a clean AAAF plot (see Fig. 6(a)). Whereas the AAAF plots start to degrade in presence of a bumper (see Fig. 6(b)) and gradually the worst AAAF plot can be seen when two paint layers are added to the bumper. It clearly shows the deterioration in angular resolution, reduction in FoV, and ambiguity in DoA when the antenna is integrated behind the painted bumper compared to antenna without in-

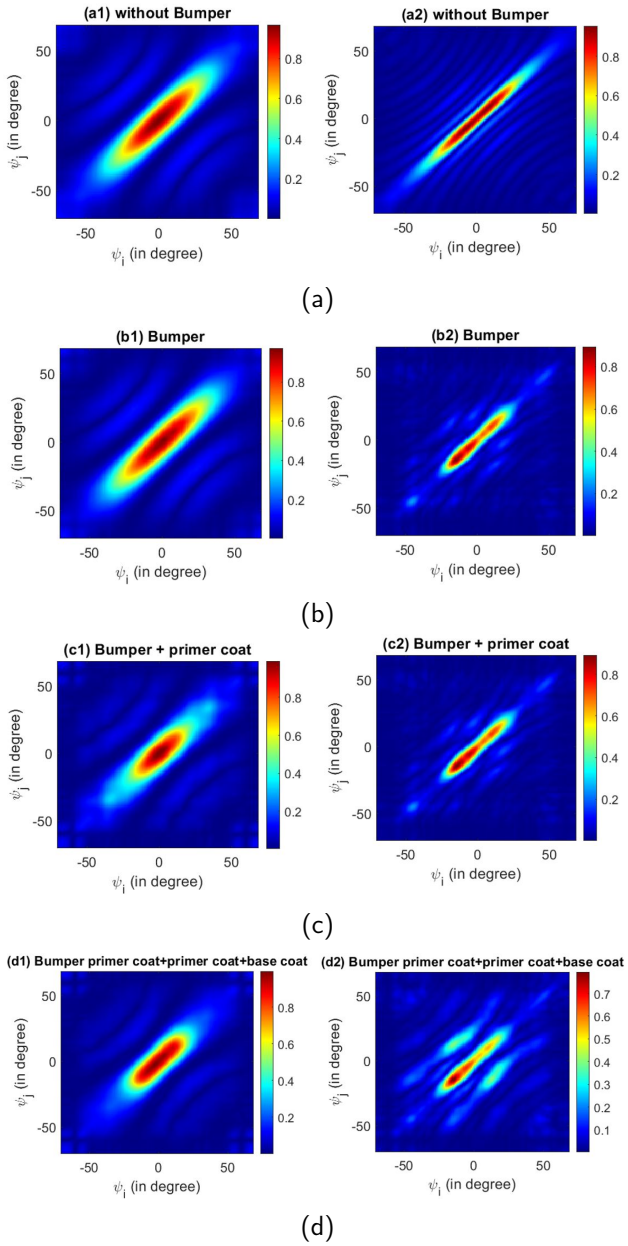

Figure 6. AAAF plots for 1D (left) and 2D (right) MIMO RADAR antennas of Fig. 1 and 2 respectively for various integration conditions at 77 GHz: (a) antenna without bumper, (b) antenna with bumper only, (c) antenna with bumper+ primer coat, and (d) antenna with bumper+ primer coat+ base coat.

tegration (Fig. 6(a)). It can be inferred from this study that the use of additional paint layers may further deteriorate the RADAR performance. A study on the effect of change in the material property (dielectric constant) of a bumper on the 1D MIMO RADAR antenna is provided in our earlier work [8].

4 Conclusion

This paper first discusses the design of a 1D and 2D MIMO RADAR antenna having 2Tx-4Rx and 3Tx-4Rx configurations respectively. It is observed that the proposed 2D MIMO RADAR provided better angular resolution in azimuth compared to the 1D counterpart. Furthermore, the 2D MIMO RADAR antenna is placed behind a painted curved bumper, and performance metrics like AAAF and antenna S-parameters are studied. It is observed that the bumper with paint material inflicts ambiguity in DoA, affects angular resolution, and alters the antenna S-parameter response over the unmounted antenna. Such studies are potentially helpful to automotive industries to obtain more insights about integrated antenna performance and to provide better solutions with high system efficiency during real-time operation.

5 Acknowledgement

Authors would like to thank Society for Innovation & Development (SID), Indian Institute of Science, Bangalore for financial support.

References

[1] J. M. Merlo and J. A. Nanzer, "A C-Band Fully Polarimetric Automotive Synthetic Aperture RADAR," *IEEE Trans. Veh. Technol.*, vol. 71, no. 3, pp. 2587-2600, March 2022.

[2] E. Marti, M. A. de Miguel, F. Garcia and J. Perez, "A Review of Sensor Technologies for Perception in Automated Driving," in *IEEE Intelligent Transportation Systems Magazine*, vol. 11, no. 4, pp. 94-108, winter 2019.

[3] M. Jokela, M. Kutila, and P. Pyykönen, "Testing and validation of automotive point-cloud sensors in adverse weather conditions," *Appl. Sci.*, vol. 9, no. 11, 2019, Art. no. 2341.

[4] J. Li and P. Stoica, "MIMO RADAR with Colocated Antennas," *IEEE Signal Processing Magazine*, vol. 24, no. 5, pp. 106-114, Sept. 2007.

[5] J. C. Dash, S. Kharche, J. Mukherjee, V. Dhoot and R. Makanaboyina, "A Model for Equivalent Loss Tangent of Multilayered Media for Automotive RADAR Applications," 2019 13th European Conference on Antennas and Propagation (EuCAP), 2019, pp. 1-4.

[6] J. C. Dash, D. Darkar and Y. Antar, "Design of Series-fed Patch Array with Modified Binomial Coefficients for MIMO RADAR Application," *2021 IEEE AP-S Symposium on Antennas and Propagation and USNC-URSI Radio Science Meeting*, 2021.

[7] J. C. Dash et al., "Performance Evaluation of Automotive RADAR in The Presence of Bumper with Multiple Paint Layers Using Bidirectional Loss Model," *2021 15th European Conference on Antennas and Propagation (EuCAP)*, 2021, pp. 1-5.

[8] J. C. Dash and D. Sarkar, “Impacts on Automotive MIMO RADAR Performance due to Permittivity Variation of Bumper Material: Insights through Bidirectional Loss and Antenna Array Ambiguity Function”, *2021 IEEE MTT-S International Microwave and RF Conference (IMARC)*, 2021, pp. 1-4.

[9] A. Di Serio, P. Hügler, F. Roos and C. Waldschmidt, "2-D MIMO RADAR: A Method for Array Performance Assessment and Design of a Planar Antenna Array," in *IEEE Transactions on Antennas and Propagation*, vol. 68, no. 6, pp. 4604-4616, June 2020.

[10] TI Application Report on MIMO RADAR: SWRA554A–May 2017–Revised July 2018. Available Online:https://www.ti.com/lit/pdf/swra554.

[11] J. C. Dash, D. Sarkar and Y. Antar,"Design of a 2D MIMO RADAR Antenna for 77 GHz Automotive Application," *IEEE International Symposium on Antennas and Propagation and USNC-URSI Radio Science Meeting*, Denver, Colorado, USA, 10-15 July. 2022.

[12] R. Z. Syeda, T. G. Savelyev, M. C. van Beurden and A. B. Smolders, "Sparse MIMO Array for Improved 3D mm- Wave Imaging RADAR," *2020 17th European RADAR Conference (EuRAD)*, 2021, pp. 342-345.

[13] Y. Xiao, F. Norouzian, E. G. Hoare, E. Marchetti, M. Gashinova and M. Cherniakov, "Modeling and Experiment Verification of Transmissivity of Low-THz RADAR Signal Through Vehicle Infrastructure," *IEEE Sensors Journal*, vol. 20, no. 15, pp. 8483-8496, 1 Aug.1, 2020.

[14] C. Vasanelli, R. Batra, A. D. Serio, F. Boegelsack and C. Waldschmidt, "Assessment of a Millimeter-Wave Antenna System for MIMO Radar Applications," *IEEE Antennas Wireless Propagation Letters*, vol. 16, pp. 1261-1264, 2017.